TELKOMNIKA Telecommunication, Computing, Electronics and Control
Vol. 18, No. 1, February 2020, pp. 552~561
ISSN: 1693-6930, accredited First Grade by Kemenristekdikti, Decree No: 21/E/KPT/2018
DOI: 10.12928/TELKOMNIKA.v18i1.13196

Design and fabrication of A Ku-band low noise amplifier using FR-4 substrate

Linh Ta Phuong[1], Bernard Journet[2], Duong Bach Gia[3]
[1]Vietnam Space Center, Ministry of Science and Technology, Vietnam
[2]LPQM (CNRS UMR-8537) École normale supérieure Paris-Saclay, CentraleSupelec, Université Paris-Saclay, France
[3]VNU University of Engineering and Technology, Hanoi, Vietnam

Article Info

Article history:

Received May 22, 2019
Revised Oct 27, 2019
Accepted Nov 30, 2019

Keywords:

FR-4
Ku-band
Low noise amplifier
Stepped impedance matching

ABSTRACT

The low noise amplifier (LNA) plays an important role in many communication systems, especially at the receiver's front-ends. In modern RF designs, The LNA is usually fabricated on a microstrip printed circuit board (PCB) due to its simplicity and ability of integrating flexibly with other components in a receiving circuitry unit. At frequencies lower than 6 GHz, the most prevalent substrate material for a microstrip LNA is FR-4 while at higher frequencies of over 10 GHz, it is challenging to design the LNA using this material without causing considerable losses to the RF signal. There are many works related to design microstrip LNA at high frequencies, however, the dielectric substrates used in most of them were high-cost materials for low dielectric loss. This paper introduces an LNA topology using the common, low-cost FR-4 substrate which can be operated in Ku-band for applications such as small satellites' receivers, with the expected noise figure of lower than 1 dB, gain of around 10 dB and the return loss of around -10 dB. The stepped impedance matching technique has been used for transmission line optimization. The simulated and measured results are presented.

Corresponding Author:

Bernard Journet,
Quantum and Molecular Photonics Laboratory, ENS Paris-Saclay,
61 Avenue du Président Wilson, 94230 Cachan, France.
Email: bernard.journet@ens-cachan.fr

1. INTRODUCTION

Low noise amplifier (LNA) has been widely applied in various communication systems, especially in the radio receiver's front-ends. Its main advantage is to amplify receiving signals which have very low amplitude to an acceptable power level that can be figured out by the receiver without causing detrimental effects to the total signal-to-noise (SNR) ratio of the receiver unit. When go through the LNA, both signal and noise are amplified, thus, the LNA is usually integrated together with a bandpass filter in order to retrieve the signal from the unwanted following noises.

For radio links such as satellite communication, the LNA of the receiver is commonly fabricated in printed circuit board (PCB) technology, in which, the Microstrip has a predominance over other types of electrical transmission line. The most popular material to used for the PCB Microstrip is the flame-retardant #4 (FR-4) epoxy glass. This dielectric material has some advantages over the others when using as a substrate for RF and PCB applications such as low cost, good mechanical properties, provides constant loss tangent over a wide band of frequencies [1]. However, the significant drawbacks of the FR-4 is its high insertion loss

at high frequencies; from the electrical performance point of view, the FR-4 is not truly a high frequency circuit material [2]. The attenuation of the RF signal (dB/inch) when running through a microstrip line can be calculated as follow [3]:

$$\alpha=2.3f \cdot tan(\delta) \cdot \varepsilon_{eff} \quad (1)$$

where:
α–Attenuation in dB / Inch.
f–Frequency in GHz
$tan(\delta)$–Loss Tangent of the material
ε_{eff}–Effective Relative dielectric constant of the material

Based on (1), for a standard FR-4 with dielectric constant ($\boldsymbol{\varepsilon_r}$)=4.35 and $tan(\delta)$=0.0023, the attenuation $\boldsymbol{\alpha}$ is 0.04 at 2 GHz and 0.2 at 10 GHz, respectively. For other material, such as Rogers RT Duroid 5880 with ($\boldsymbol{\varepsilon_r}$)=2.2 and $tan(\delta)$=0.0004, this value is about 0.004 at 2 GHz and 0.02 at 10 GHz, respectively. Furthermore, E.L.Holzman showed that for microstrip parallel-coupled resonator using FR-4 substrate with a dielectric constant of 4.5, the insertion loss ($\boldsymbol{S_{21}}$) increased rapidly from 2 GHz to 15 GHz [4], as illustrated in Figure 1.

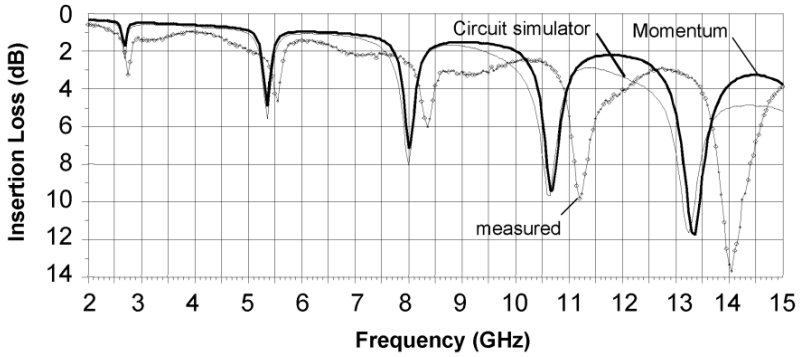

Figure 1. The measured insertion loss of microstrip parallel-coupled resonator versus simulated insertion loss of Advanced Design System (ADS) [4]

It is clearly seen from Figure 1 that the increase of S_{21} is about 3.5 dB from 2 GHz to 15 GHz, this is even more drastically when comparing the S_{21} at the resonant frequency of 2.7 GHz (around 1.9 dB) with that of 13.4 GHz (around 11.9 dB). These results show that when using the FR-4, it is really challenging to design an LNA of over 10 GHz without causing significant attenuation to the signal. To avoid the ambiguity in terminology, the S_{21} parameter hereby can be understood as insertion loss for non-amplifying circuits and as gain for amplifying circuits, both are measured in dB. The others S-parameters, $\boldsymbol{S_{11}}$ and $\boldsymbol{S_{22}}$, are the input return loss and output return loss of the 2-port network.

There are previous works related to research, design and fabricate the LNA using FR-4, but only limited in the frequency range of under 6 GHz: J. Rajendral and R. Peter (2014) [5] designed an L-band LNA using the ATF-58143 high electron mobility transistor for RF front end, with a moderate gain of about 13 dB and input return loss of 10 dB in the frequency range between 0.9 and 1.5 GHz. M.Arsalan and F.Wu [6] demonstrated a novel implementation of a pHEMT LNA that can be applied to satellite communications tracking receiver. The LNA has one stage, working between frequency span of 2-2.2 GHz with the transducer gain of over 10 dB. A wideband, three cascaded LNA worked in L-band and S-band has been presented by J.Lv et al. [7], in which, a novel equalization was proposed and demonstrated. This LNA, due to the effect of the equalization, attained an impressive high gain in the operating frequency range, about 38 dB, while the input and out return losses are approximately 7 dB and 8 dB, respectively. M. Z. A. A. Aziz et al. [8] developed a single stage low noise amplifier circuit design for the frequency band of 5 GHz to 6 GHz, with the gain of around 7.78 dB in the whole span, the $\boldsymbol{S_{11}}$ of below-10 dB from 5.5 GHz to 6 GHz. G. L. Ning et al. [9] presented a design of concurrent LNA for multi-band applications, in which, a 2 cascaded common-source staged LNA is matched by stepped-impedance transformers. By using this technique, the gain and input return loss over the whole designed frequency band of 2–6 GHz are around 21 dB and 10 dB, respectively.

There are also some LNA designs at X-band and over, but none using FR-4: Girlando et al. [10] presented a LNA topology for X-band and the beginning of Ku-band based on the 46 GHz-f_T pure bipolar technology, with the gains of 11.5 dB and 8 dB at 8 GHz and 12 GHz, respectively. C. Wang [11] introduced a wideband LNA using noise neutralizing technique, which is expected to apply to 3–10 GHz ultrawideband system. This topology had a gain of around 12 dB, with very good gain flatness from 2 GHz to 10 GHz. However, the gain values decreased rapidly at frequencies over 12 GHz, thus, this topology cannot cover the Ku-band.

The scope of our work is to design and fabricate a microstrip LNA using FR-4 that can be integrated to Ku-band receiver front-ends, especially for small satellite (SmallSat) applications, where low cost and short lead time are two inseparable factors of the SmallSat development. For details, the FR-4 material can be experimentally used instead of traditional high frequency materials, thus offering major cost reduction. Moreover, the design procedure and technique are being simplified in order to easily produce in any radiocommunications laboratory, as well as apply to mass-production for small satellites' testing and performance assurance at subsystem level [12]. This paper is organized as follows: section 2 is the introduction of technology used for the amplifier's active device and impedance matching technique, as well as the design and simulation of the proposed LNA. The experimental results are demonstrated in section 3 and the conclusions are drawn in section 4.

2. DESIGN AND SIMULATION RESULTS OF THE LOW NOISE AMPLIFER

The desired LNA has one stage only, the block diagram is shown in Figure 2. There are various technologies used in designing the active device for the LNA at Ku-band: Deng et al. [13], Afshar et al. [14], M. Yamagata and H. Hashemi [15], Liou et al. [16] developed the X/Ku-band LNA topologies based on the CMOS technology. The *GaAs* MESFET was demonstrated in the LNA designs of Bashir et al. [17], Islam et al. [18]. Furthermore, LNAs using high electron mobility transistor (HEMT) were reported in the journals of M. Fallahnejad and A. Kashaniniya [19] and Shoaib et al. [20]. A two-staged Ku-band LNA for satellite applications was presented by P. Bishoyi and S. S. Karthikeyan [21]. F. Guo and Z. Yao designed a *GaN* LNA in order to compare the power handling of their module with that of the traditional *GaAs* LNA [22].

The measured results of these works will be shown in the next section. In this design, we used hetero junction field effect transistor (HJFET), and the NE3515S02 model has been chosen. Though providing middle output power, the NE3515S02's advantages are very low noise figure and high associated gain. This FET is a suitable choice for LNA or buffer amplifiers from X to Ku-band. In our case, for DC biasing, we chose the DC operation point (bias point) at V_{DS} = 2V, I_D = 40mA in order to keep the device in its active region. The corresponding gate to source voltage V_{GS} is -0.2V and the corresponding power dissipation is less than 150 mW.

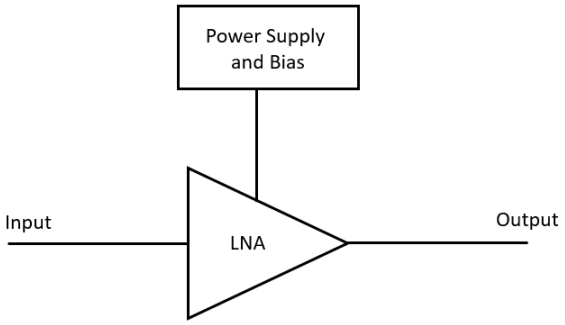

Figure 2. The block diagram of the proposed LNA

In general, the advantages of JFET technology is exhibiting very high input resistance and low output resistance, providing high thermal stability and high degree of isolation between the input and output of the transistor. It is a good choice for microstrip LNA, with respect to the impedance matching aspect. In order to deliver the maximum amount of power from the source to the load, the input and output impedances (Z_{in} and Z_{out}) of the transistor need to be matched with the source and load impedances (Z_S and Z_L). We do the impedance matching for the standard Z_S and Z_L of 50 Ohms. The figure below demonstrates the LNA with matching network.

In Figure 3, Γ_S, Γ_L, Γ_{in} and Γ_{out} are the reflection coefficients of the source, the load, the input and out put of the transistor, respectively. Z_0 is the characteristic impedance of the transmission lines which are connected to the source and the load, in our case, its value is 50Ω. When goes through the input and output matching networks, the Z_0 is transformed to the corresponding complex impedances of the transistor's input and output. G_S, G_0 and G_L are the gain factors of the input matching network, the transistor itself and the output matching network in turn. The overall transducer gain is $G_T=G_S.G_0.G_L$. Since G_0 is unique at a certain frequency of a given transistor, the overall gain of the amplifier is only being controlled by varying the values of G_S and G_L of the impedance matching networks [24]. The impedance matching technique used for this LNA topology is stepped impedance matching. This is a method in which, the impedance values changed flexibly from the input to the output of the impedance matching network. It can be easily applied to the microstrip PCB by changing the width and length of the microstrip transmission lines. By using stepped impedance matching, the physical length of the transmission lines can be shortened, thus decrease the attenuation of the RF signal when travelling through these. This point is very important when fabricating the microwave circuits with high attenuation substrate like FR-4. Furthermore, the operation bandwidth of the LNA can be improved when applying this matching technique and the dimensions of the circuit can be considerably reduced. Figure 4 illustrates a typical stepped impedance transformer.

In Figure 4, impedance of the i^{th} stage that looks toward the termination can be calculated as follow [9]:

$$Z_i' = Z_i \frac{Z_{i+1}' + jZ_i \tan(\beta l_i)}{Z_i + jZ_{i+1}' \tan(\beta l_i)} \quad (2)$$

where i = 1,2,….,n and β is the propagation constant. l_i is the physical length and Z_i is the characteristic impedance of the i^{th} stage. In general, the principle in designing our stepped impedance transformer is similar to that of [25], but for a much higher frequency range.

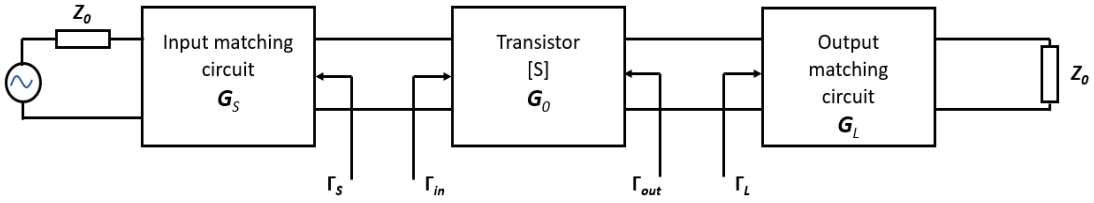

Figure 3. The block diagram of the single stage LNA with matching network (redrawn from [23])

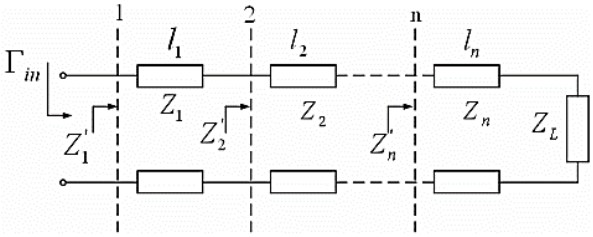

Figure 4. Principal diagram of the stepped impedance transformer [9]

For impedance matching, the input and output reflection coefficients (S_{11} and S_{22}) of NE3515S02 at the chosen frequencies in Ku-band was taken from the device's datasheet, based on these values, the input and output impedances of the transistor can be calculated. Consequently, by using (2) recursively, the characteristic impedances Z_i of each stepped impedance section can be determined. The electrical length of each section has been chosen equal to a quarter wavelength or a multiple of this value, thus the LNA can be operated in several frequency ranges in the Ku-band. The corresponding physical length and width of each section can then be calculated, as showed in Table 1.

It is noticed in the above tables that the dimensions of the stepped impedance transformers varied nonlinearly over the four sections. This allowed us to versatilely modify the impedance values through each section, thus change the values of the corresponding quality factor (Q) of them. For details, when degrading

the quality factor, the gain decreased but a wider bandwidth has been reached, and vice versa. Consequently, the bandwidth can be adjusted (narrower or wider) with respect to the design requirement of the LNA. The FR-4 material used for the LNA has the following characteristics: Relative dielectric constant: 4.34, loss tangent: 0.0023, dielectric height: 1.6 mm, conductor thickness: 0.035 mm, roughness: 0.0095. The simulated results (in Decibel) of the input reflection coefficient (S_{11}) and insertion loss (S_{21}) have been executed by the Advanced Design System (ADS) 2014, provided by Keysight. The schematic design is illustrated in Figure 5.

Table 1. The design values of stepped impedance transformer for the input and output branch matching

Section	Input branch			Output branch		
	Width (mm)	Length (mm)	Z_i (Ohms)	Width (mm)	Length (mm)	Z (Ohms)
1	3.87	7.22	43.9	3.87	5.32	43.9
2	9.8	2.12	22.4	7.68	2.12	27.1
3	5.8	11.5	33.3	5.8	10.46	33.3
4	2.75	4.03	54	2.6	10.1	55.8

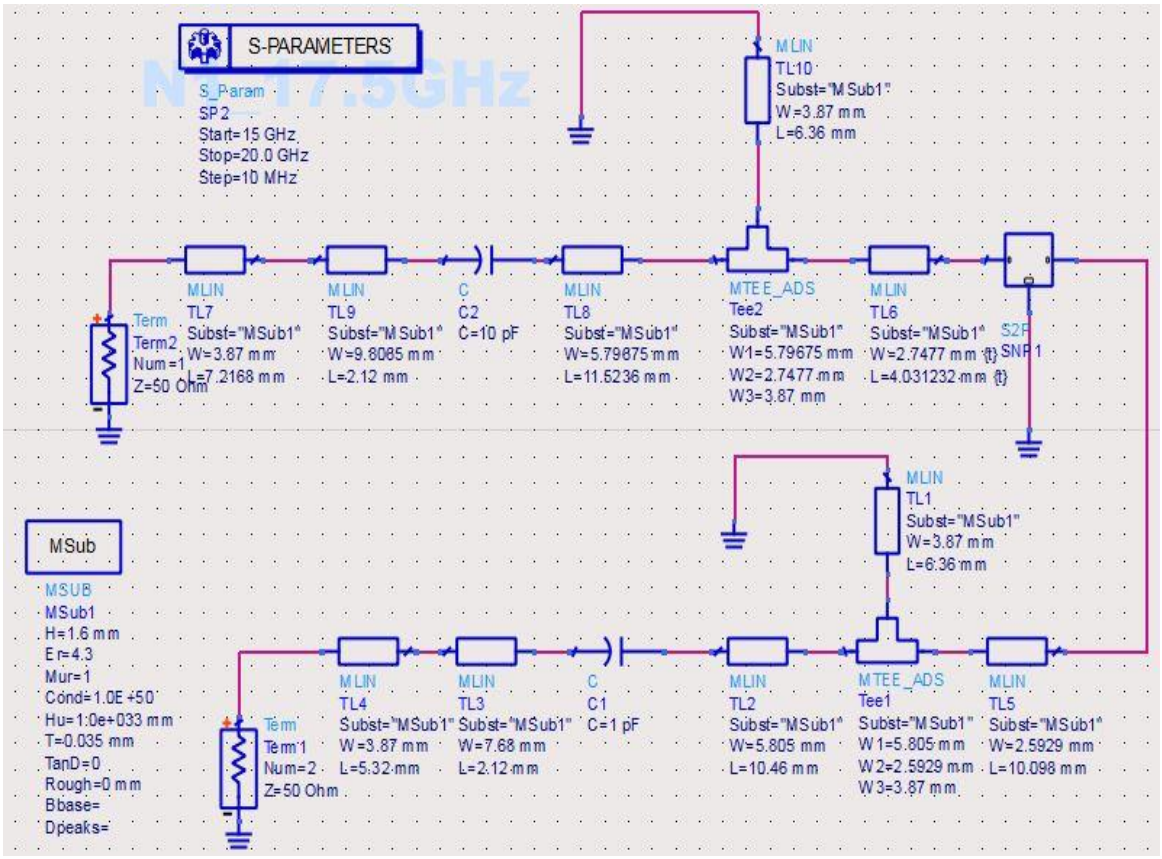

Figure 5. The simulation schematic of the Ku-band LNA using FR-4, with stepped impedance matching network

Figure 6 shows the simulated results of the gain and return loss of the proposed LNA in 3 frequency ranges, centered at 12.2 GHz, 14.9 GHz and 17.6 GHz, respectively. It is clearly seen that in the above figures, the S_{21} and S_{11} is approximately 11.9 dB and-18 dB at 12.2 GHz, 12.5 dB and-24 dB at 14.9 GHz and around 9.5 dB and-9 dB at 17.6 GHz. It means that our LNA has the ability of operating in several frequency ranges from the beginning to the end of the Ku-band. Figure 7 shows the simulated results of the noise figure (in dB) in the 3 mentioned frequency ranges. As can be seen in the above figure, the noise figures of all the mentioned frequency ranges are below 1 dB. The simulated results met the design requirement, thus, the noise is predicted to have no detrimental effect to the designed LNA.

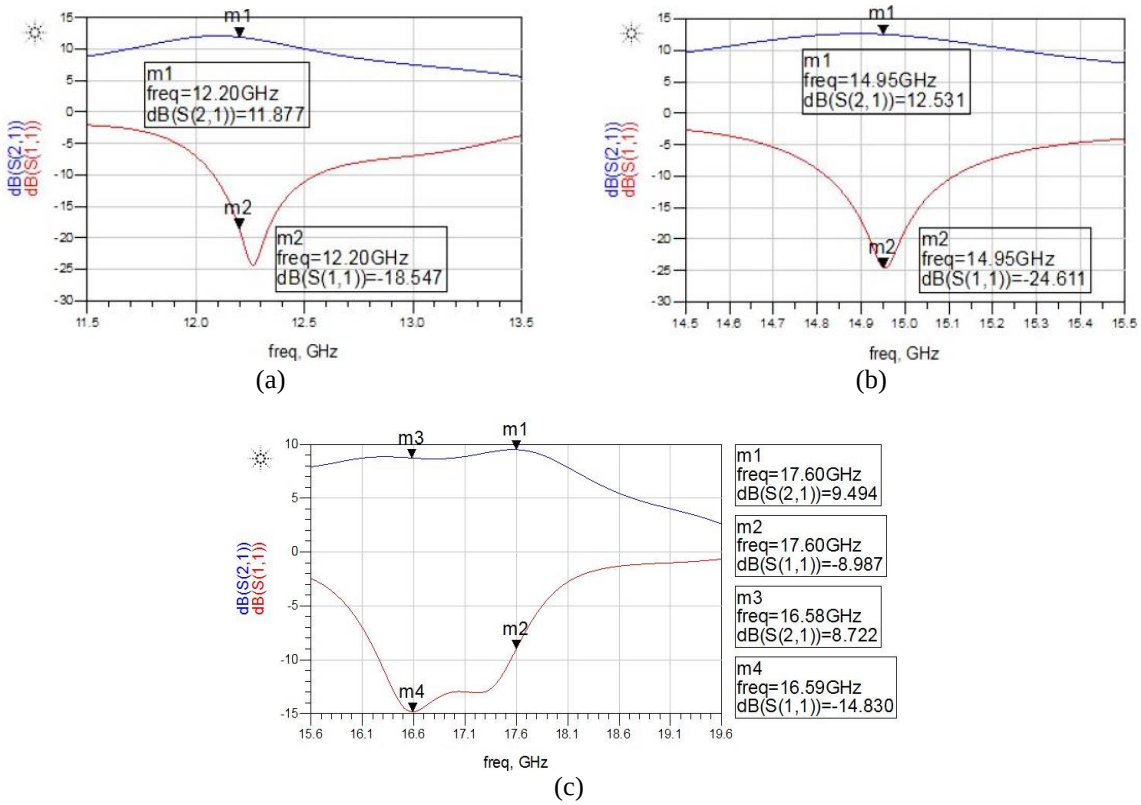

Figure 6. The simulated results of S_{11} and S_{21} in the frequency range of (a) 11–14 GHz (b) 14–16 GHz (c) 16–19 GHz

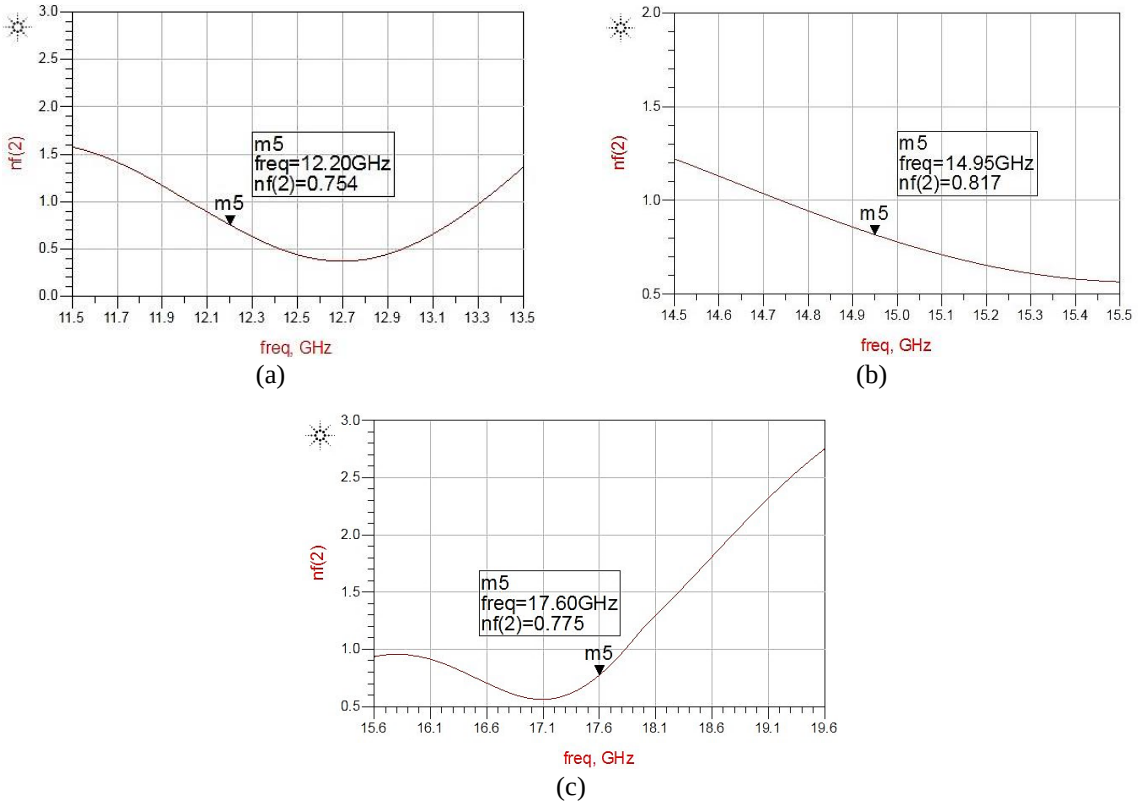

Figure 7. The simulated result of the noise figure seen from the input in the frequency ranges which centered at (a) 12.2 GHz, (b) 14.9 GHz, (c) 17.6 GHz

3. MEASURED RESULTS

The LNA circuit was designed and fabricated in our laboratory based on the ADS package and the LPKF ProtoMat C40 machine. For testing and measuring, the Agilent E8257D Signal Generator has been used to provide an incoming signal to the input of the LNA module, the Agilent E4446A Spectrum Analyzer then received the output signal of the LNA and displayed it in the frequency domain, as shown in Figure 8. Figure 9 shows the measured results of the Ku-band LNA, which are corresponding to the above simulated results. The measured frequency ranged from 12 GHz to 18 GHz. The measure was done by collecting the amplitude values of the receiving signal over the measured frequency ranges with the frequency step of 10 MHz.

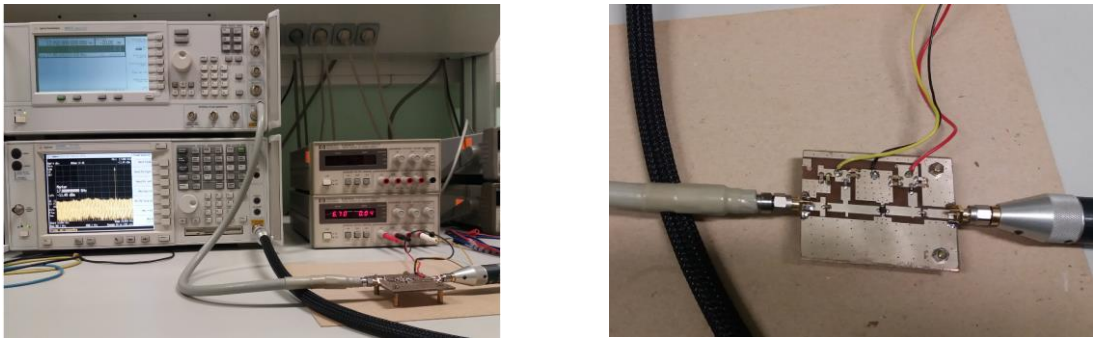

(a) (b)

Figure 8. (a) The experimental measurement, (b) The fabricated LNA

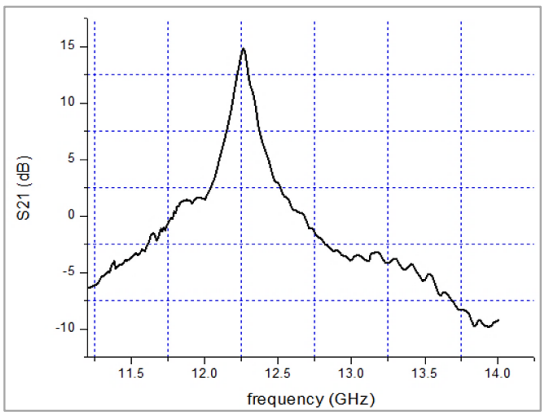

(a)

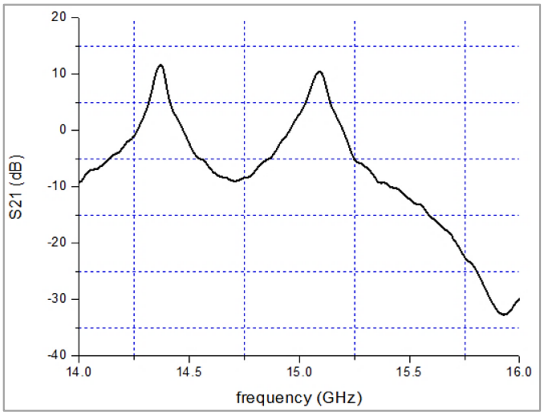

(b)

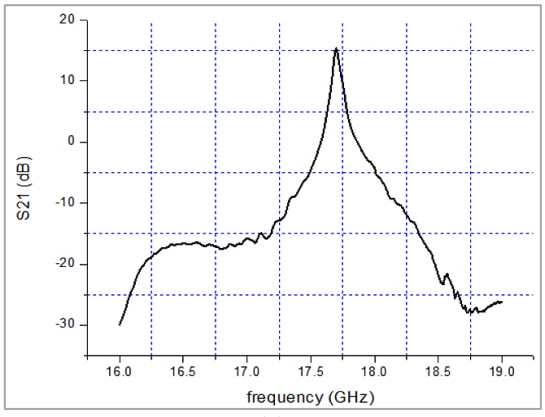

(c)

Figure 9. The measured results of S_{21} in the frequency range of
(a) 11–4 GHz, (b) 14–16 GHz, (c) 16–19 GHz

In Figure 9 (a), the frequency is about 12.2 GHz, which is well-matched with the above prediction. The -10 dB bandwidth is approximately 400 MHz, which is narrower than that of the simulated result. However, the peaked gain is considerably higher (15 dB compared with 11.9 dB). As can be seen in Figure 9 (b), in the frequency region of 14–16 GHz, the gain values have two maxima of around 11 dB and 10 dB at the frequencies of 14.37 GHz and 15.15 GHz, respectively. This result is different from the S_{21} curve in Figure 6 (b), it mainly caused by the attenuation effect of the FR-4 substrate in real environment. However, the highest gain values at these frequencies are acceptable.

Like the two above experimental results, the trend of the S_{21} curve in Figure 9 (c) showed a more selective characteristic than the simulated result. The measured gain is approximately 10 dB at 17.8 GHz, which is almost similar to the simulation. The frequency bandwidth is being tightened as predicted in the previous section. The measured -10 dB bandwidth is around 200 MHz. The trade-off between gain and bandwidth is also being illustrated in Figure 9 (a) and Figure 9 (b). Table 2 shows the comparison between our purposed LNA and the LNA's previous works.

Table 2. Comparison of the design parameters of proposed LNA and other LNAs operate in Ku-band

References	Technology	Frequencies (GHz)	Gain (dB)	Note
This work	HJFET	12.2 14.4 and 15.1 17.6	15 10 15	Demonstration for narrowband frequencies
Bashir et. al. [17]	*GaAs* MESFET	12 GHz	14.2	Simulation results only
Islam et. al. [18]	*GaAs* MESFET	12 GHz	8.9	
M.Fallahnejad, A.Kashaniniya [19]	HEMT	10 GHz 15 GHz	13 15	Simulation results only
Shoaib et. al. [20]	PHEMT	12.7 GHz	8.4	
Deng et. al. [13]	CMOS (0.18μm)	14 to 15	>10	
B.Afshar, A.M. Niknejad [14]	CMOS (0.18μm)	11 GHz	12 (2 stages) 8 (single stage)	
Liou et. al. [16]	CMOS (0.18μm)	12 15 (midband) 18	10.1 9.7 8.2	
M.Yamagata, H.Hashemi [15]	CMOS (0.13μm)	10.1	13-14	

In general, the average S_{21} of our work from 12 GHz to 18 GHz is not as good as that of the mentioned works. This is due to the fact that our fabricated substrate is FR-4, a high attenuation material at the frequencies of over 10 GHz, thus our topology can hardly be used as a wideband LNA at the Ku-band. However, when zooming in the narrow frequency spans with the center frequencies demonstrated above, the measured gains are well suited for the narrowband LNA's applications. In this case, the gain flatness is not a major parameter as it does in the wideband LNA. Furthermore, the narrowband gains can be easily tuned to the desired center frequencies in the whole Ku-band by modifying the stepped impedance transmission lines.

4. CONCLUSION

This paper introduced about a Ku-band low noise amplifier using the common FR-4 substrate. By using this type of material, we can primarily solve out the problem of balancing between cost and performance of the high frequency LNA. Furthermore, by applying the stepped impedance matching technique, the circuit's length is significantly reduced and it leads to the ability of integrating this with small receiver's modules, such as the receiver front-ends of the small satellites. The simulated and measured results are being presented, and the gain values over the experimental frequency ranges are approximated to the maximum gain value of the NE3515S02 HJFET's datasheet in Ku-band. Though there were some differences of the peaked gain at lower frequency ranges between simulation and measurement, it still proved that the proposed LNA module can be operated as a narrowband amplifier in the entire Ku-band with high selective frequency, and the bandwidth can be flexibly adjusted with respect to the design requirement by varying the transmission lines' dimensions of the impedance matching network.

REFERENCES

[1] A. R. Djordjevic, R. M. Biljie, V. D. Likar-Smiljanic and T. K. Sarkar, "Wideband frequency-domain characterization of FR-4 and time-domain causality," *IEEE Transactions on Electromagnetic Compatibility*, vol. 43, no. 4, pp. 662-667, Nov 2001.

[2] J. Coonrod, et. al., "Selecting PCB Materials for High-Frequency Applications," *Microwave Engineering Europe*, pp. 18-21, 2012.
[3] Rick Hartley, "RF/Microwave PC Board Design and Layout Base Materials for High Speed, High Frequency PC Boards," [Online], Available: http://www.eas.uccs.edu/~mwickert/ece5250/notes/RFMicrowave-PCB-Design-and-Layout.pdf
[4] E. L. Holzman, "Wideband measurement of the dielectric constant of an FR4 substrate using a parallel-coupled microstrip resonator," *IEEE Transactions on Microwave Theory and Techniques*, vol. 54, no. 7, pp. 3127-3130, July 2006.
[5] J. Rajendran, R. Peter, "Design and simulation of low noise amplifier for RF front end at L band," *First International Conference on Computational Systems and Communications (ICCSC)*, Trivandrum, pp. 86-89, 2014.
[6] M. Arsalan and F. Wu, "An S band tracking receiver LNA for satellite communications," *2018 International Workshop on Antenna Technology (iWAT)*, Nanjing, pp. 1-4, 2018.
[7] Juncai Lv, Yongfang Bao, Jiurong Huang, "Wideband low noise amplifier using a novel equalization," *2016 Progress in Electromagnetic Research Symposium (PIERS)*, Shanghai, pp. 609-614, 2016.
[8] M. Z. A. A. Aziz, J. Din, M. K. A. Rahim, "Low noise amplifier circuit design for 5 GHz to 6 GHz," *RF and Microwave Conference*, Selangor, Malaysia, pp. 5-8, 2004.
[9] G. L. Ning, Z. Y. Lei, L. J. Zhang, R. Zou, L. Shao., "Design of concurrent low-noise amplifier for multi-band applications," *Progress In Electromagnetics Research C*, Marrakesh, Morocco, vol. 22, pp. 165-178, 2011.
[10] G. Girlando, G. Ferla, E. Ragonese and G. Palmisano, "Silicon bipolar LNAs in the X and Ku bands," *9th International Conference on Electronics, Circuits and Systems*, Dubrovnik, Croatia, vol. 1, pp. 113-116, 2002.
[11] C. Wang and C. Wang, "A 90nm CMOS Low Noise Amplifier Using Noise Neutralizing for 3.1-10.6 GHz UWB System," *2006 Proceedings of the 32nd European Solid-State Circuits Conference*, Montreux, pp. 251-254, 2006.
[12] M. N. Sweeting, "Modern Small Satellites-Changing the Economics of Space," *Proceedings of the IEEE*, vol. 106, no. 3, pp. 343-361, March 2018.
[13] K. Deng, et al., "A Ku-band CMOS low-noise amplifier," *2005 IEEE International Workshop on Radio-Frequency Integration Technology: Integrated Circuits for Wideband Comm & Wireless Sensor Networks*, Singapore, pp. 183-186, 2005.
[14] B. Afshar and A. M. Niknejad, "X/Ku Band CMOS LNA Design Techniques," *IEEE Custom Integrated Circuits Conference 2006*, San Jose, CA, pp. 389-392, 2006.
[15] M. Yamagata and H. Hashemi, "A Differential X/Ku-Band Low Noise Amplifier in 0.13-μm CMOS Technology," *IEEE Microwave and Wireless Components Letters*, vol. 17, no. 12, pp. 888-890, Dec 2007.
[16] Wan-Rone Liou, Siddarth Rai Mahendra and Tsung-Hsing Chen, "A wideband LNA design for Ku-Band applications," *2010 International Conference on Communications, Circuits and Systems (ICCCAS)*, Chengdu, pp. 680-684, 2010.
[17] M. A. Bashir, M. M. Ahmed, U. Rafique and Q. D. Memon, "Design of a Ku-band high gain low noise amplifier," *2013 IEEE International RF and Microwave Conference (RFM)*, Penang, pp. 168-171, 2013.
[18] M. R. Islam et al., "Design of a low noise amplifier with GaAs MESFET at Ku_Band," *International Conference on Computer and Communication Engineering (ICCCE'10)*, Kuala Lumpur, pp. 1-5, 2010.
[19] M. Fallahnejad and A. Kashaniniya, "Design of Low Noise Amplifiers at 10 GHZ and 15 GHZ for Wireless Communication Systems," *IOSR Journal of Electrical and Electronics Engineering*, vol. 9, no. 5, pp. 47-53, Jan 2014.
[20] N. Shoaib, M. Ahmad and I. Mahmood, "Design, fabrication & testing of Low Noise Amplifier at Ku-Band," *2008 2nd International Conference on Advances in Space Technologies*, Islamabad, pp. 18-23, 2008.
[21] P. Bishoyi and S. Karthikeyan, "Design of a two stage Ku band low noise amplifier for satellite applications," *2015 International Conference on Communications and Signal Processing (ICCSP)*, Melmaruvathur, pp. 0270-0273, 2015.
[22] F. Guo and Z. Yao, "Design of a Ku-band AlGaN/GaN low noise amplifier," *Proceedings of 2014 3rd Asia-Pacific Conference on Antennas and Propagation*, Harbin, pp. 1406-1408, 2014.
[23] D. M. Pozar, "Microwave Engineering," Third Edition, New York: John Willey and Son, pp. 610, 2005.
[24] G. Gonzalez, "Microwave Transistor Amplifiers: Analysis and Design," Second Edition, New Jersey: Prentice Hall. pp. 228-229, 1997.
[25] K. Inderkumar, et. al., "Compact wideband quarter-wave transformer using stepped impedance microstrip lines," *2017 2nd International Conference on Communication Systems, Computing and IT Applications (CSCITA)*, Mumbai, pp. 184-188, 2017.

BIOGRAPHIES OF AUTHORS

Linh Ta Phuong received the M.Sc. Degree in Electronics and Telecommunications Technology from University of Engineering and Technology, Vietnam National University in 2014 and M.Sc. Degree in Aerospace Engineering from Tohoku University in 2017. From 2015 up to now, he is a researcher in Vietnam National Space Center, Vietnam Academy of Science and Technology. His researches mainly focus on microwave engineering, communications in satellites, ground station and radio systems.
Email: tplinh@vnsc.org.vn

Bernard Journet was born in Lyon, France in 1956. From 1983 to 1984, he was a teacher of the 1st year BTS Electronics class and 1st year Mechanics and Automatism class of Gustave Eiffel Highschool. From 1984 to 1989, he was a teacher of the BTS class of Optics and Precision and TF10 in the Fresnel High School. He has been an Associate Professor at the department of Electronics, Electrotechniques and Automatic (EEA) of the ENS Paris-Saclay, France from Oct.1, 1989 up to now. His field of research focuses on Optoelectronic Oscillator and Applications for Optical and Microwave systems.
Email: bernard.journet@ens-cachan.fr

Duong Bach Gia was born in Ha Dong Dist., Hanoi, Vietnam in 1950. He received the B.S degree in radio physics in 1972 and the Ph.D. degree in wireless physics from University of Hanoi in 1988. From 1988 to 1990, he was a researcher assistant in Leningrad University, Russia. From 1991 to 2005, he was a researcher in academy of air force. He has been a lecturer and head of electronics and telecommunications center, University of Engineering and Technology, Vietnam National University since 2006. He was promoted to Associate Professor in 2009 and to Professor in 2016. His research focuses on RF analog signal processing, RF chip design, radar engineering and technology, automatic control.
Email: duongbg@vnu.edu.vn